

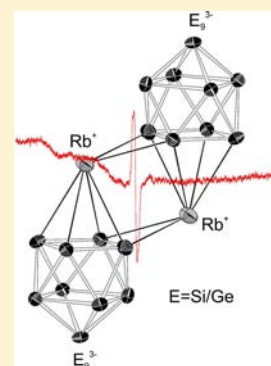
Mixed Si/Ge Nine-Atom Zintl Clusters: ESI Mass Spectrometric Investigations and Single-Crystal Structure Determination of Paramagnetic $[\text{Si}_{9-x}\text{Ge}_x]^{3-}$

Markus Waibel and Thomas F. Fässler*

Department Chemie, Technische Universität München, Lichtenbergstraße 4, D-85747 Garching, Germany

Supporting Information

ABSTRACT: Mixed Si/Ge compounds are of special interest as potential materials for photovoltaic applications. In order to evaluate the usage of soluble precursor compounds, we investigated the synthesis of heteroatomic nine-atom clusters that consist of Si and Ge atoms through dissolution of the ternary Zintl phases $\text{K}_{12}\text{Si}_{17-x}\text{Ge}_x$ ($x = 9, 12$) and $\text{Rb}_{12}\text{Si}_{17-x}\text{Ge}_x$ ($x = 9$). Electrospray ionization (ESI) mass spectrometry demonstrates the presence of mixed $\text{Si}_{9-x}\text{Ge}_x$ clusters in acetonitrile solution. From ammonia solutions of the ternary phases, four compounds that contain 3-fold negatively charged $[\text{Si}_{9-x}\text{Ge}_x]^{3-}$ clusters are obtained. The paramagnetic behavior is confirmed by EPR spectroscopy. $[\text{E}_9]^{3-}$ Zintl clusters are considered as intermediate structures in the stepwise oxidation of $[\text{E}_9]^{4-}$ clusters to novel element allotropes ($\text{E} = \text{Si-Pb}$). The structure of $\text{Rb}[\text{Rb-crypt}]_2[\text{Si}_{2.3(1)}\text{Ge}_{6.7(1)}](\text{NH}_3)_7$ and the isostructural structures of $[\text{Rb-crypt}]_3[\text{Si}_{2.2(1)}\text{Ge}_{6.8(1)}](\text{NH}_3)_8$, $[\text{K-crypt}]_3[\text{Si}_{2.4(1)}\text{Ge}_{6.6(1)}](\text{NH}_3)_{8.5}$, and $[\text{K-crypt}]_3[\text{Si}_{4.6(1)}\text{Ge}_{4.4(1)}] \cdot (\text{NH}_3)_{8.5}$ are investigated by single-crystal X-ray diffraction (crypt = 4,7,13,16,21,24-hexaoxa-1,10-diazabicyclo[8.8.8]-hexacosane). The Si/Ge ratio of the products correlates with the composition of the ternary precursor phases.



INTRODUCTION

Doping of silicon with germanium enhances the properties for application of inorganic Si-based solar cells due to a considerably lower band gap,¹ and the synthesis of soluble precursor compounds that are composed of covalently connected Si and Ge atoms is a promising approach.^{2–4} In this context, we investigate the nature of homoatomic $[\text{E}_9]^{4-}$ Zintl clusters ($\text{E} = \text{Si-Pb}$) whose syntheses (in solution and solid state), structure, and description of the bonding situation within the polyanionic cluster subunit are well understood.^{5–9} The clusters exist with different negative charges and less charged clusters correspond to formal oxidation products of the $[\text{E}_9]^{4-}$ species. In analogy to Wade's rules, the structure of the monocapped square antiprisms (C_{4v} point group symmetry) $[\text{E}_9]^{4-}$ can be described as a *nido*-type cluster having $2n + 4 = 22$ skeletal electrons per cluster unit.^{5–11} Corresponding *closo*-type $[\text{E}_9]^{2-}$ Zintl clusters ($\text{E} = \text{Si-Pb}$) with $2n + 2 = 20$ skeletal electrons adopt the shape of a tricapped trigonal prism with D_{3h} symmetry.^{5–9} Since $[\text{E}_9]^{3-}$ Zintl clusters ($\text{E} = \text{Si-Pb}$) arise with 21 electrons, their structures can be regarded as an intermediate between the *closo*- and the *nido*-type structures. Paramagnetic 21-electron Zintl clusters may exist as isolated $[\text{E}_9]^{3-}$ Zintl clusters ($\text{E} = \text{Si-Pb}$) with a singly occupied LUMO (lowest unoccupied molecular orbital).^{8,9} These clusters are free radicals and have exclusively been isolated as crypt salts (crypt = 4,7,13,16,21,24-hexaoxa-1,10-diaza-bicyclo[8.8.8]-hexacosane) from solutions of A_4E_9 and $\text{A}_{12}\text{Si}_{17}$ Zintl phases ($\text{A} = \text{K, Rb}$) in ethylenediamine or liquid ammonia.^{8,9} Their paramagnetic behavior was measured for the $[\text{Si}_9]^{3-}$ clusters in solution,¹² while a detailed study and an additional exploration

of the bulk magnetism of the cluster compounds was carried out for $\text{E} = \text{Ge-Pb}$.¹³ Powdered samples of $[\text{K-crypt}]_6\text{E}_9\text{E}_9(\text{en})_{1.5}\text{to}_{0.5}$ ($\text{E} = \text{Ge-Pb}$) showed increasing line widths of the EPR signals from Ge to Pb.¹³ An alternative to “formally” achieve 21 electrons per nine-atomic cluster unit is the oxidative coupling of two $[\text{E}_9]^{4-}$ subunits ($\text{E} = \text{Si-Pb}$). This leads to a dimeric unit with one *exo*-cluster bond, as it is experimentally known for the polyanions $[\text{Ge}_9\text{-Ge}_9]^{6-}$ and $[\text{Sn}_9\text{-Sn}_9]^{6-}$.^{14–18}

In principle, all isolated $[\text{E}_9]^{3-}$ clusters ($\text{E} = \text{Si-Pb}$) as well as the oxidatively coupled dimeric units like $[\text{Ge}_9\text{-Ge}_9]^{6-}$ and $[\text{Sn}_9\text{-Sn}_9]^{6-}$ can be regarded as intermediate structures in the stepwise oxidation of $[\text{E}_9]^{4-}$ clusters to their element structures. Further oxidation leads to trimeric $[\text{Ge}_9\text{=Ge}_9\text{=Ge}_9]^{6-}$,^{19,20} tetrameric $[\text{Ge}_9\text{=Ge}_9\text{=Ge}_9\text{=Ge}_9]^{8-}$,^{21,22} or polymeric $^{1}_{\infty}[-\text{Ge}_9-]^{2-}$ ^{23,24} fragments of this element. A series of various Ge allotropes built up via oxidation of Ge_9 units has been theoretically predicted.^{9,25} Element modifications of germanium with clathrate-II or mesoporous structure made from $[\text{Ge}_9]^{4-}$ have been obtained experimentally.^{26–28}

Recently, the isolation of diamagnetic mixed $[\text{Si}_{4-x}\text{Ge}_x]^{4-}$ and $[\text{Si}_{9-x}\text{Ge}_x]^{4-}$ clusters from ammonia solutions of ternary phases of the *nominal* composition $\text{A}_{12}\text{Si}_{17-x}\text{Ge}_x$ ($\text{A} = \text{K, Rb}$) has been described.^{2–4} Here, we report on the solubility of mixed $\text{Si}_{9-x}\text{Ge}_x$ clusters in acetonitrile as demonstrated by electrospray ionization (ESI) mass spectrometry. Additionally,

Received: December 20, 2012

Published: April 29, 2013

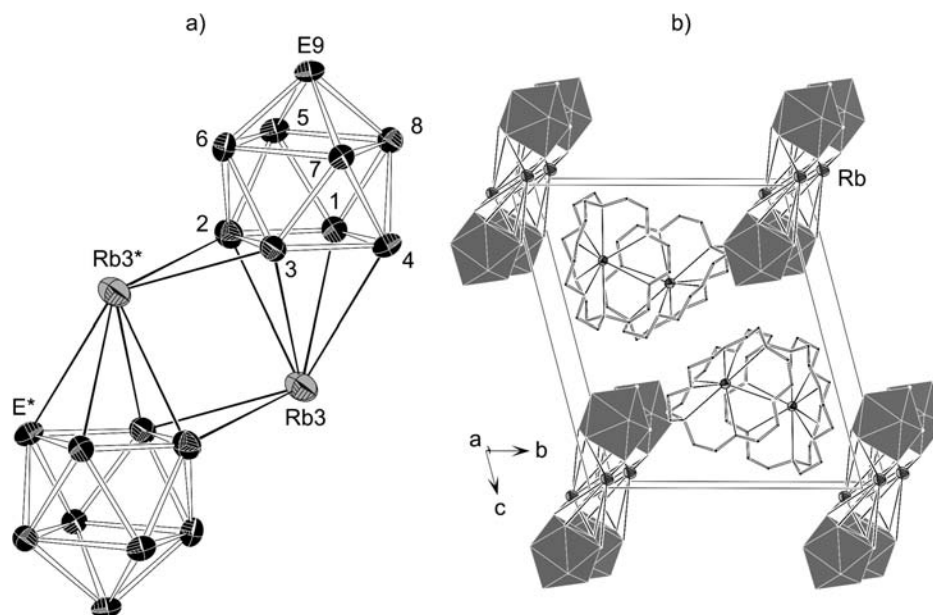


Figure 1. (a) Structure of the heteroatomic polyanion **1a**. Two bridging Rb3 atoms interconnect two of the heteroatomic polyanions **1a**. Displacement ellipsoids were measured at 120 K and are drawn at the 70% probability level. Ge amounts at atomic sites E in % (standard deviation): E1 20.2(5), E2 57.6(5), E3 87.2(5), E4 88.8(5), E5 90.5(5), E6 83.0(5), E7 85.9(5), E8 79.6(5), E9 90.0(5). (b) Unit cell of **1**. Heteroatomic clusters are shown as gray polyhedra; displacement ellipsoids of Rb atoms were measured at 120 K and are drawn at the 70% probability level. Crypt molecules are shown schematically, and ammonia molecules of crystallization are omitted for clarity. $[\text{Rb}_2[\text{Si}_{2.3(1)}\text{Ge}_{6.7(1)}]_2]^{4-}$ dimers with two bridging Rb atoms are aligned along the *a* direction.

we report on the synthesis and structural characterization of the first mixed paramagnetic clusters $[\text{Si}_{9-x}\text{Ge}_x]^{3-}$ ($x = 4.4, 6.6, 6.7,$ and 6.8). These clusters possess an unpaired electron and are stable as monomers, while dimeric units in analogy to $[\text{Ge}_9-\text{Ge}_9]^{6-}$ have not been observed so far.^{14–17} The paramagnetic nature is confirmed by EPR spectroscopy, and the composition of the 3-fold negatively charged Si–Ge clusters is influenced by the Si/Ge ratio of the precursor phases.

RESULTS AND DISCUSSION

Ternary phases of nominal composition $\text{A}_{12}\text{Si}_{17-x}\text{Ge}_x$ ($\text{A} = \text{K}, \text{Rb}; x = 1, 5, 9, 12$) or $\text{A}_4\text{Si}_2\text{Ge}_2$ ($\text{A} = \text{K}, \text{Rb}$) can be obtained by heating the elements in sealed tantalum containers.^{2,3} On the basis of their isotopic relationship to binary alkali silicides $\text{A}_{12}\text{Si}_{17}$ ($\text{A} = \text{Na}-\text{Cs}$),^{12,29} comparable powder X-ray diagrams with Bragg reflections shifted to lower angles in 2θ result for $\text{A}_{12}\text{Si}_{17-x}\text{Ge}_x$.^{2,3} As an example, the powder diagram of $\text{K}_{12}\text{Si}_8\text{Ge}_9$ is depicted in Figure S1 in the Supporting Information. Some of the reaction products appear as mixtures of $\text{K}_{12}\text{Si}_8\text{Ge}_9$, $\text{A}_4\text{Si}_{4-x}\text{Ge}_x$,³ and α -Si (see Figures S2 and S3 in the Supporting Information for $\text{K}_{12}\text{Si}_5\text{Ge}_{12}$ and $\text{Rb}_{12}\text{Si}_8\text{Ge}_9$, respectively), as has been reported before also for the ternary Zintl phase $\text{K}_6\text{Rb}_6\text{Si}_{17}$.³⁰

The solubility of the solids $\text{A}_{12}\text{Si}_{17-x}\text{Ge}_x$ ($\text{A} = \text{K}, \text{Rb}; x = 1, 5, 9, 12$) in liquid ammonia was meanwhile investigated by dissolving mixtures including the ternary Zintl phase $\text{Rb}_{12}\text{Si}_{12}\text{Ge}_5$. As we have shown recently, these experiments led to the isolation of two 4-fold negatively charged clusters $[\text{Si}_{9-x}\text{Ge}_x]^{4-}$ ($x = 1.2, 1.5$), present in the crystals of $[(\text{Rb}-18\text{-crown-6})\text{Rb}_3][\text{Si}_{7.5(1)}\text{Ge}_{1.5(1)}](\text{NH}_3)_4$ and $\text{Rb}_4\text{Si}_{7.8(1)}\text{Ge}_{1.2(1)}(\text{NH}_3)_5$, respectively.² The resulting clusters adopt the shape of a monocapped square antiprism with the Ge atoms being mostly located at the open face of the cluster. As the Si/Ge ratio at the different atom sites in $[(\text{Rb}-18\text{-crown-6})\text{Rb}_3][\text{Si}_{7.5(1)}\text{Ge}_{1.5(1)}](\text{NH}_3)_4$ and $\text{Rb}_4\text{Si}_{7.8(1)}\text{Ge}_{1.2(1)}(\text{NH}_3)_5$

differs significantly, a superposition of homoatomic $[\text{Si}_9]^{4-}$ and $[\text{Ge}_9]^{4-}$ clusters has been obviated.² The Si/Ge ratio was found to slightly deviate from the composition of the precursor since a more Ge-rich phase, $\text{A}_4\text{Si}_{4-x}\text{Ge}_x$, was observed as a byproduct in $\text{Rb}_{12}\text{Si}_{12}\text{Ge}_5$.²

Given that Cu complexes can be used to isolate $[\text{Si}_4]^{4-}$ and $[\text{Ge}_9]^{4-}$ clusters from solution,^{30,31} also the reactivity of the heteroatomic phases $\text{A}_{12}\text{Si}_{17-x}\text{Ge}_x$ ($\text{A} = \text{K}, \text{Rb}$) toward organometallic compounds was investigated. Using similar reaction conditions, dissolution of the ternary phase $\text{Rb}_{12}\text{Si}_8\text{Ge}_9$ in liquid ammonia in the presence of crypt and the addition of Cy_3PCuCl yielded $\text{Rb}[\text{Rb-crypt}]_2[\text{Si}_{2.3(1)}\text{Ge}_{6.7(1)}](\text{NH}_3)_7$ (**1**), which contains the 3-fold negatively charged heteroatomic polyanion $[\text{Si}_{2.3(1)}\text{Ge}_{6.7(1)}]^{3-}$ (**1a**, see Figure 1a). Due to the presence of α -Si as a byproduct in $\text{Rb}_{12}\text{Si}_8\text{Ge}_9$, the Ge amount in **1a** is higher than in the precursor used for the synthesis (see Figure S3 in Supporting Information).

Figure 1a shows cluster **1a**, which appears as a monocapped square antiprism with evident distortion from C_{4v} symmetry, as visible from the ratio of the diagonal lengths of the open square face of the antiprism ($d_1 = \text{Si}/\text{Ge}1-\text{Si}/\text{Ge}3 = 3.451(2)$ Å; $d_2 = \text{Si}/\text{Ge}2-\text{Si}/\text{Ge}4 = 3.841(2)$ Å; $d_2/d_1 = 1.11$). The distortion toward C_{2v} symmetry is thus much more pronounced than in the recently reported heteroatomic compound $\text{Rb}_4\text{Si}_{7.8(1)}\text{Ge}_{1.2(1)}(\text{NH}_3)_5$ that contains $[\text{Si}_{7.8(1)}\text{Ge}_{1.2(1)}]^{4-}$ with a d_2/d_1 ratio of 1.03.² This trend has already been observed before for homoatomic $[\text{E}_9]^{n-}$ clusters ($n = 3, 4; \text{E} = \text{Si}-\text{Pb}$).⁸

Crystals of **1** contain three Rb atoms per 3-fold negatively charged heteroatomic polyanion $[\text{E}_9]^{3-}$ (**1a**, $\text{E} = \text{Si}/\text{Ge}$). Each of the Rb1 and Rb2 atoms is coordinated by a crypt molecule (see Figure 1b). The third Rb3 atom coordinates in an η^4 manner to the open square face of the cluster and to ammonia molecules of crystallization. Furthermore, the Rb3 atoms build a bridge in η^2 coordination to a second heteroatomic cluster **1a*** (Figure 1a). This structural motif is unique for 3-fold

negatively charged group 14 element clusters. So far, all homoatomic $[E_9]^{3-}$ ($E = \text{Si-Pb}$) clusters were isolated exclusively as crypt salts without direct interactions between the cationic and the corresponding polyanionic cluster units.⁸

In order to confirm the existence of mixed clusters in solution, we dissolved a second sample of the Ge-rich phase $\text{Rb}_{12}\text{Si}_8\text{Ge}_9$ in liquid ammonia and investigated the acetonitrile extract after evaporation of ammonia. The ESI mass spectrum of this extract confirms the presence of mixed clusters as clearly indicated by the rather typical isotope distribution of the anions as shown for the mass with the highest abundance at $m/z = 943$ in Figure 2. The mass peak matches $[\text{Rb}_2\text{Si}_{12}\text{Ge}_6]^-$ and

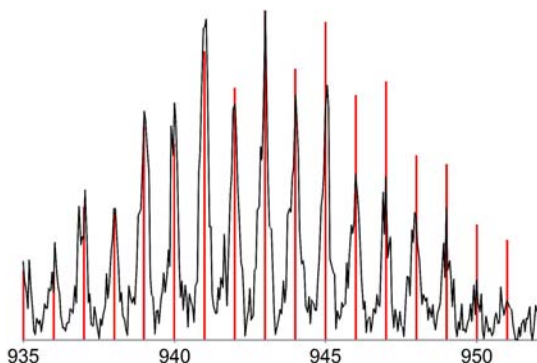


Figure 2. Section of the ESI mass spectrum of an acetonitrile solution of $\text{Rb}_{12}\text{Si}_8\text{Ge}_9$. The experimental mass distribution for $[\text{Rb}_2\text{Si}_{12}\text{Ge}_6]^-$ is depicted in black; the theoretical masses of the isotope distribution are in red.

corresponds to two mixed Si_6Ge_3 clusters that are attached to two Rb atoms, a unit as it occurs for example in crystals of compound **1** (Figure 1a).

Further investigations on the reactivity of the ternary $\text{A}_{12}\text{Si}_{17-x}\text{Ge}_x$ ($A = \text{K, Rb}$) alloys toward Cu and Rh complexes resulted in compounds for which the crystal structures contain mixed Zintl ion clusters isostructural to the reported polysilicide salt $[\text{K-crypt}]_3\text{Si}_9(\text{NH}_3)_8$, which contains a 3-fold negatively charged $[\text{Si}_9]^{3-}$ cluster.¹² Through dissolution of the ternary phase $\text{Rb}_{12}\text{Si}_8\text{Ge}_9$ in the presence of crypt and $[\text{Rh}(\text{cod})\text{Cl}]_2$ crystals of the salt $[\text{Rb-crypt}]_3[\text{Si}_{2.2(1)}\text{Ge}_{6.8(1)}]-(\text{NH}_3)_8$ (**2**) became accessible. Again, the comparably high amount of Ge in crystal structure **2** is caused by the presence of α -Si as a byproduct in $\text{Rb}_{12}\text{Si}_8\text{Ge}_9$ (see Figure S3 in Supporting Information).

$[\text{K-crypt}]_3[\text{Si}_{2.4(1)}\text{Ge}_{6.6(1)}](\text{NH}_3)_{8.5}$ (**3**) crystallizes from an ammonia solution of $\text{K}_{12}\text{Si}_5\text{Ge}_{12}$, crypt, and Ph_3PCuCl , while $[\text{K-crypt}]_3[\text{Si}_{4.6(1)}\text{Ge}_{4.4(1)}](\text{NH}_3)_{8.5}$ (**4**) was obtained from $\text{K}_{12}\text{Si}_8\text{Ge}_9$ in the presence of crypt, MesCu , and Ph_3P . Here, the Si/Ge ratio of the products almost perfectly matches the one of the precursors (compare Table 1). The 3-fold negatively charged heteroatomic polyanions $[\text{Si}_{9-x}\text{Ge}_x]^{3-}$ ($x = 6.8$ for **2a**, 6.6 for **3a**, 4.4 for **4a**; as an example the structure of **4a** is shown in Figure S8 in Supporting Information) in crystals of **2**, **3** and

4, respectively, are each surrounded by three alkali metal atoms (Rb in case of **2**, K in cases of **3** and **4**). All alkali metals in **2**, **3**, and **4** are coordinated by crypt molecules (as an example, the unit cell of **4** is shown in Figure 3). The polyanions **2a**, **3a**, and **4a** can be described as C_{2v} -distorted monocapped square antiprisms ($d_1/d_2 = 1.12$ for **2a**, $d_1/d_2 = 1.11$ for **3a**, and $d_1/d_2 = 1.13$ for **4a**);

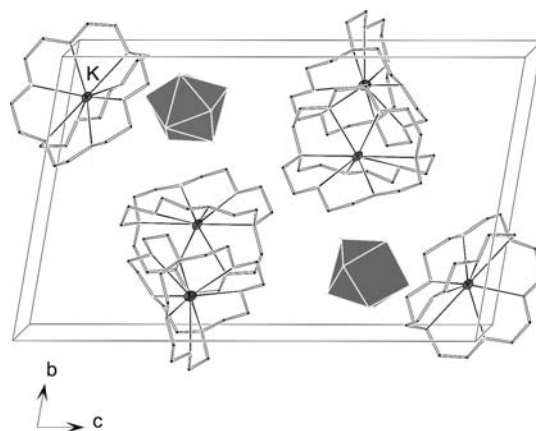


Figure 3. Unit cell of **4**. Heteroatomic clusters are shown as gray polyhedra; displacement ellipsoids of the K atoms were measured at 120 K and are drawn at the 70% probability level. Crypt molecules are shown schematically, and ammonia molecules of crystallization are omitted for clarity.

The Ge amount has been determined crystallographically for the different atomic sites of the clusters **1a–4a** and is graphically shown in Figure 4 (see also Experimental Section

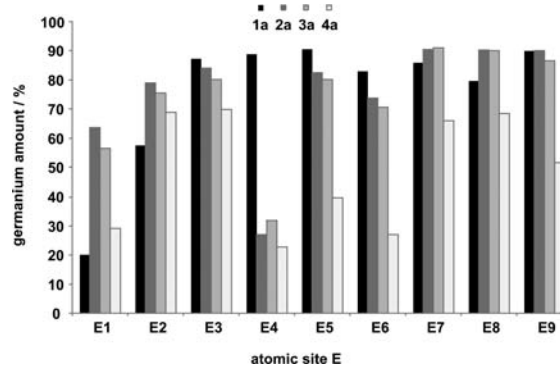


Figure 4. The amount of Ge at the various atomic sites E in $[\text{E}_9]^{3-}$ clusters ($E = \text{Si/Ge}$).

for **2a** and **3a** and Figure S8 in Supporting Information for **4a**). Interestingly, the Si/Ge ratio of all $[\text{E}_9]^{3-}$ clusters (**1a–4a**) is varying depending on the ratio of the ternary precursor phase that has been used for the synthesis (for details see Table 1). In the cases of **1** and **2**, the precursor phase contains α -Si as an

Table 1. Comparison of the Si/Ge Ratio in Precursors and Resulting $[\text{E}_9]^{3-}$ Clusters

crystal structure	$[\text{Si}_{2.3}\text{Ge}_{6.7}]^{3-}$ (1a)	$[\text{Si}_{2.2}\text{Ge}_{6.8}]^{3-}$ (2a)	$[\text{Si}_{2.4}\text{Ge}_{6.6}]^{3-}$ (3a)	$[\text{Si}_{4.6}\text{Ge}_{4.4}]^{3-}$ (4a)
Ge amount/%	74	76	73	51
precursor	$\text{Rb}_{12}\text{Si}_8\text{Ge}_9^a$	$\text{Rb}_{12}\text{Si}_8\text{Ge}_9^a$	$\text{K}_{12}\text{Si}_5\text{Ge}_{12}^b$	$\text{K}_{12}\text{Si}_8\text{Ge}_9$
Ge amount in polyanionic substructure/%	53	53	71	53

^a α -Si as impurity. ^bContains $\text{K}_4\text{Si}_{4-x}\text{Ge}_x^3$ as a byproduct.

impurity (see Figure S3 in Supporting Information). As a consequence of the insolubility of α -Si in liquid ammonia, the polyanions **1a** and **2a** contain a higher amount of Ge. The heteroatomic ternary phases used for the preparation of **3** and **4** contain either no impurity or an $A_3Si_{4-x}Ge_x$ ($A = K, Rb, x = 1-4$)³ phase with approximately the same Si/Ge ratio as the $A_{12}Si_{17-x}Ge_x$ ($A = K, Rb$) phase under consideration (see Figures S1 and S2 in the Supporting Information).³ The corresponding polyanions **3a** and **4a** exhibit the same Si/Ge ratio as their precursor. By contrast, the $Rb_{12}Si_8Ge_9$ sample used for ESI mass spectrometry contains a Ge-rich $Rb_4Si_{4-x}Ge_x$ phase (insoluble in solvents like acetonitrile or liquid ammonia). Consequently, Si-rich $[Rb_2Si_{12}Ge_6]^-$ clusters are present in the ESI mass spectrum. Summing up, the Si/Ge ratio of the products directly depends on the composition of the precursor, which is essential for application in materials with defined band gaps.

Since all mixed Si–Ge nine-atom clusters appear with three counterions per cluster, they possess an odd number of thus paramagnetic.^{5–9} EPR spectroscopy was applied to prove the paramagnetic nature of the heteroatomic polyanions $[E_9]^{3-}$ (**1a–4a**, $E = Si/Ge$) and to rule out the presence of hydrogenated species like $[HE_9]^{3-}$ ($E = Si/Ge$). Comparable $[HSn_9]^{3-}$ clusters have already been detected in ethylenediamine solutions of K_4Sn_9 .³² Since all compounds immediately decompose at ambient temperature due to a loss of ammonia, we recorded an EPR spectrum (see Figures S4, S5, and S6 in the Supporting Information) of a solid residue that contained crystals of compound **3** prepared by evaporation of ammonia from a solution of $K_{12}Si_5Ge_{12}$, crypt, and Ph_3PCuCl . Further, the residue of a similarly obtained ammonia solution was redissolved in pyridine, and after filtration, the EPR spectrum of the frozen pyridine solution was recorded at 150 K (Figure 5).

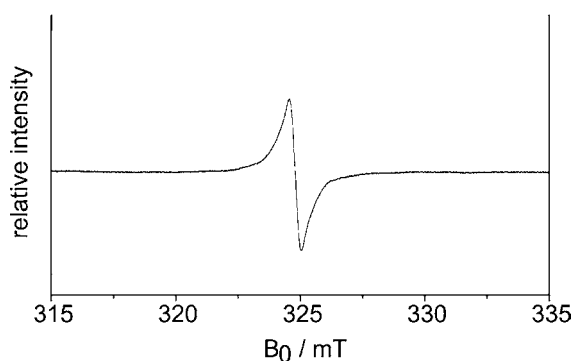


Figure 5. X-band EPR spectrum at 150 K ($g = 2.004(2)$) of **3**.

Both EPR spectra exhibit a strong signal with a g value of 2.004(2) and a line width of approximately 3 mT. All known paramagnetic and homoatomic $[E_9]^{3-}$ ($E = Ge-Pb$) clusters show either isotropic or anisotropic EPR signals with comparable g values.^{9,13,33–37} The line width of the here described spectra compares well with the characteristics of paramagnetic $[Ge_9]^{3-}$,¹³ while the g value of 2.004 is the same as reported for $[Si_9]^{3-}$ clusters.¹² For $E = Si$, EPR activity of a pyridine solution is reported; however neither the line width nor the error of the g value of the EPR signal is described in detail.¹² The EPR signal in Figure 5 (as well as in Figure S4 in Supporting Information) shows a g value comparable to $[Si_9]^{3-}$ but a line width related to that of $[Ge_9]^{3-}$. Paramagnetic Cu^{II} species, present for example in the solid precursor PPh_3CuCl

after subsequent oxidation, show completely different EPR spectra (see Figure S7 in Supporting Information). Therefore, it can be excluded that the EPR signal originates from paramagnetic Cu^{II} impurities. The mixed radical ions **1a–4a** can be regarded as polyhedral Wade clusters with 21 skeletal electrons. According to the sensitivity and the low crystalline yield, compounds **1–4** elude from other spectroscopic investigations or further magnetic measurements.

CONCLUSION

The series of 3-fold negatively charged $[Si_9-xGe_x]^{3-}$ clusters shows that also heteroatomic radicals can be handled in solution, and an evident characterization via X-ray diffraction, EPR spectroscopy, and ESI mass spectrometry is possible. The isolation of clusters with different Ge amounts ($x = 4.4, 6.6, 6.7, 6.8$) shows that the Si/Ge ratio of the products is influenced by the compositions of the precursors, all of which show a homogeneous distribution of both elements. This enables their applicability as starting material for the formation of semi-conducting materials. The paramagnetic clusters reported here were isolated from solutions containing also transition metal complexes, whereas diamagnetic $[Si_9]^{4-}$ clusters are obtained directly from solutions of the precursor phases.^{38,39} Though also examples with diamagnetic $[E_9]^{4-}$ ($E = Si, Si/Ge$) clusters isolated in the presence of transition metal complexes are known in the literature,^{2,30} the discussion on their role as oxidants is still ongoing.

EXPERIMENTAL SECTION

General. All experiments were carried out under an argon atmosphere using standard Schlenk and glovebox techniques. Ph_3PCuCl , Cy_3PCuCl , $MesCu$, and $[Rh(cod)Cl]_2$ were prepared according to the literature.^{40–46} Crypt was dried *in vacuo*. Liquid ammonia was dried and stored over sodium metal.

Precursor Synthesis. The ternary Zintl phases $K_{12}Si_{17-x}Ge_x$ ($x = 9, 12$) and $Rb_{12}Si_{17-x}Ge_x$ ($x = 9$) were synthesized from mixtures of 6.52 mmol potassium or rubidium and the relative molar ratio of Si and Ge in sealed tantalum containers. This mixtures were heated to 900 °C for 1 h and cooled to room temperature at a rate of 0.1 °C/min.²

Powder X-Ray Diffraction. Phase analyses of $K_{12}Si_{17-x}Ge_x$ ($x = 9, 12$) and $Rb_{12}Si_{17-x}Ge_x$ ($x = 9$) were carried out using a Stoe STADI P diffractometer (Ge(111) monochromator; $Cu K\alpha$ radiation) equipped with a linear position-sensitive detector. The products were finely ground in an agate mortar and filled into sealed glass capillaries. The samples were measured in Debye–Scherrer mode ($2\theta_{max} = 60^\circ$). Data analysis was performed using the Stoe WinXPOW software package.⁴⁷

Single-Crystal Structure Determination. The thermally, at ambient temperature, very unstable air and moisture sensitive crystals of **1**, **2**, **3**, and **4** were transferred from the reaction solution into perfluoropolyalkyl ether oil at 213 K under a cold N_2 stream. The single crystals were fixed on a glass capillary and positioned in a 120 K cold N_2 stream using the crystal cap system. Data collection at 120(2) K: Bruker APEX II diffractometer mounted at a window of a rotating anode FR 591 (Mo $K\alpha$ radiation) in the case of **3**; Oxford-Diffraction Xcalibur3 diffractometer (Mo $K\alpha$ radiation) in cases of **1**, **2**, and **4**. Structures were solved by direct methods (SHELXS-97)⁴⁸ and refined by full-matrix least-squares calculations against F^2 (SHELXL-97).⁴⁹ During the refinement cycles, the positions and atomic displacement parameters (ADPs) for Si and Ge were set equal at each atom site of the tetrel cluster. The occupation ratio has been checked for each individual position within the cluster by applying particular free variables.² This procedure is commonly used for refining solid-state compounds with mixed site occupation. The Si occupation at each atom site in **1a**, **2a**, **3a**, and **4a** significantly differs, and consequently

the coexistence of homoatomic $[\text{Si}_9]^{3-}$ and $[\text{Ge}_9]^{3-}$ clusters can be ruled out. Since the interatomic distances between nearest neighbor atoms in $[\text{Si}_9]^{3-}$ and $[\text{Ge}_9]^{3-}$ clusters differ only slightly and even overlap (2.404(3)–2.690(2) Å for the $[\text{Si}_9]^{3-}$ cluster and 2.509(2)–2.873(2) Å for the $[\text{Ge}_9]^{3-}$ cluster), the maxima of the electron density related to a Si atom next to a Ge atom will fall below the resolution of the X-ray diffraction experiment. The resolution is further lowered due to the relatively large anisotropic displacement parameters. As an example, the overlap of a $[\text{Si}_9]^{3-}$ and a $[\text{Ge}_9]^{3-}$ cluster with equivalent orientations and center of mass positions is shown in the Supporting Information (Figure S8). Intrinsic occupational disorder at the atomic positions within the clusters generally leads to less diffracting crystals compared to their homoatomic analogs, resulting in data with comparably lower resolution.

Electron Dispersive X-Ray (EDX) Analysis. EDX analysis of the crystals of **1**, **2**, **3**, and **4** was carried out on a JEOL-SEM 5900LV spectrometer and confirmed the approximate percentage of Rb/Si/Ge in compounds **1** and **2** and of K/Si/Ge in compounds **3** and **4**, as well as the absence of other elements heavier than Na.

EPR Spectroscopy. EPR spectroscopic investigations were carried out at ambient temperature and at 150 K using a JEOL JES-FA 200 spectrometer at the X-band frequency ($\nu \sim 9.07$ GHz, modulation 0.4 mT). For the spectrum shown in Figure S4 in the Supporting Information, single crystals of **3** and the residue of the reaction of $\text{K}_{12}\text{Si}_5\text{Ge}_{12}$, crypt, and Ph_3PCuCl obtained after evaporation of ammonia were transferred into an EPR tube inside a glovebox and fused under inert gas. Furthermore, the residue was dissolved in pyridine and subsequently filtered into a second fused silica EPR tube under an inert gas atmosphere. The spectrum is shown in Figure 5. The g values were standardized to signals of the Mn standards.

ESI Mass Spectrometry. After dissolution of $\text{Rb}_{12}\text{Si}_8\text{Ge}_9$ (100 mg; 0.052 mmol) in 1 mL of liquid ammonia at -78 °C, the ammonia was subsequently evaporated. The remaining sample was dissolved in 1 mL of acetonitrile and after filtration directly measured using a Varian 500 mass spectrometer operating with an electrospray ionization technique and an ion detection in the negative mode. Details for the measurement: spray shield voltage, -600 V; capillary voltage, -80 V; exit lens voltage, $+10$ V; focus lens voltage, $+35$ V; needle voltage, -5000 V; drying gas temperature, 350 °C.

Compound 1. $\text{Rb}_{12}\text{Si}_8\text{Ge}_9$ (143 mg; 0.075 mmol), crypt (51 mg, 0.135 mmol), and $\text{C}_7\text{H}_7\text{PCuCl}$ (28.5 mg, 0.075 mmol) were weighed into a Schlenk tube and dissolved in approximately 1 mL of liquid ammonia at -78 °C. The resulting brown suspension, still containing an insoluble, not further characterized residue, was kept at -70 °C. **1** crystallized as orange blocks after several weeks with approximately 5% yield. Crystal size: $0.2 \times 0.1 \times 0.05$ mm³; unit cell parameters: $a = 13.9539(3)$, $b = 15.7757(4)$, $c = 17.1535(3)$ Å, $\alpha = 74.690(2)^\circ$, $\beta = 86.490(2)^\circ$, $\gamma = 66.190(2)^\circ$, $V = 3327.65(12)$ Å³; triclinic, space group $P\bar{1}$ (No. 2), $Z = 2$, $\rho_{\text{calcd}} = 1.68$ g cm⁻³, $\mu = 5.3$ mm⁻¹, $\theta_{\text{max}} = 26.25^\circ$, 55 121 measured reflections, 13 423 independent reflections, $R_{\text{int}} = 0.057$, $R_1 = 0.037$ and $wR_2 = 0.084$ for reflections with $I > 2\sigma(I)$, $R_1 = 0.072$ and $wR_2 = 0.089$ for all data.

Compound 2. $\text{Rb}_{12}\text{Si}_8\text{Ge}_9$ (143 mg; 0.075 mmol), crypt (51 mg, 0.135 mmol), and $[\text{Rh}(\text{cod})\text{Cl}]_2$ (18.5 mg, 0.0375 mmol) were weighed into a Schlenk tube and dissolved in approximately 1 mL of liquid ammonia at -78 °C. The resulting brown suspension, still containing an insoluble, not further characterized residue, was kept at -70 °C. **2** crystallized as a few very small orange blocks after 19 weeks. Crystal size: $0.1 \times 0.1 \times 0.08$ mm³; unit cell parameters: $a = 14.1713(5)$, $b = 15.1574(6)$, $c = 22.9195(9)$ Å, $\alpha = 80.251(3)^\circ$, $\beta = 84.862(3)^\circ$, $\gamma = 66.630(4)^\circ$, $V = 4452.6(3)$ Å³; triclinic, space group $P\bar{1}$ (No. 2), $Z = 2$, $\rho_{\text{calcd}} = 1.55$ g cm⁻³, $\mu = 4.0$ mm⁻¹, $\theta_{\text{max}} = 25.00^\circ$, 44 245 measured reflections, 15 574 independent reflections, $R_{\text{int}} = 0.142$, $R_1 = 0.062$ and $wR_2 = 0.085$ for reflections with $I > 2\sigma(I)$, $R_1 = 0.172$ and $wR_2 = 0.104$ for all data. Si amounts at atomic sites E in % (standard deviation): E1 63.6(5), E2 79.0(6), E3 84.1(6), E4 27.1(6), E5 82.5(6), E6 73.8(5), E7 90.4(6), E8 90.2(5), E9 90.1(6).

Compound 3. $\text{K}_{12}\text{Si}_5\text{Ge}_{12}$ (111 mg; 0.075 mmol), crypt (51 mg, 0.135 mmol), and Ph_3PCuCl (27 mg, 0.075 mmol) were weighed into a Schlenk tube and dissolved in approximately 1 mL of liquid ammonia

at -78 °C. The resulting brown suspension, still containing an insoluble, not further characterized residue, was kept at -70 °C. **3** crystallized as a few red blocks after 32 weeks. Crystal size: $0.2 \times 0.2 \times 0.1$ mm³; unit cell parameters: $a = 14.1637(8)$, $b = 15.1827(8)$, $c = 22.9666(13)$ Å, $\alpha = 80.043(2)^\circ$, $\beta = 84.853(3)^\circ$, $\gamma = 66.496(2)^\circ$, $V = 4460.8(2)$ Å³; triclinic, space group $P\bar{1}$ (No. 2), $Z = 2$, $\rho_{\text{calcd}} = 1.44$ g cm⁻³, $\mu = 2.4$ mm⁻¹, $\theta_{\text{max}} = 25.00^\circ$, 139 916 measured reflections, 15 617 independent reflections, $R_{\text{int}} = 0.138$, $R_1 = 0.055$ and $wR_2 = 0.133$ for reflections with $I > 2\sigma(I)$, $R_1 = 0.088$ and $wR_2 = 0.144$ for all data. Si amounts at atomic sites E in % (standard deviation): E1 56.4(4), E2 75.5(4), E3 80.2(4), E4 31.9(4), E5 80.1(4), E6 70.7(4), E7 91.0(4), E8 90.1(4), E9 86.5(4).

Compound 4. $\text{K}_{12}\text{Si}_8\text{Ge}_9$ (101 mg; 0.075 mmol), crypt (51 mg, 0.135 mmol), MesCu (14 mg, 0.075 mmol), and Ph_3P (20 mg, 0.075 mmol) were weighed into a Schlenk tube and dissolved in approximately 1 mL of liquid ammonia at -78 °C. The resulting brown suspension, still containing an insoluble, not further characterized residue, was kept at -70 °C. **4** crystallized as a few orange blocks after 19 weeks. Crystal size: $0.2 \times 0.2 \times 0.1$ mm³; unit cell parameters: $a = 14.1056(5)$, $b = 15.1430(4)$, $c = 22.8797(6)$ Å, $\alpha = 80.150(2)^\circ$, $\beta = 84.792(2)^\circ$, $\gamma = 66.546(3)^\circ$, $V = 4415.9(2)$ Å³; triclinic, space group $P\bar{1}$ (No. 2), $Z = 2$, $\rho_{\text{calcd}} = 1.39$ g cm⁻³, $\mu = 1.8$ mm⁻¹, $\theta_{\text{max}} = 25.00^\circ$, 41 512 measured reflections, 15 300 independent reflections, $R_{\text{int}} = 0.095$, $R_1 = 0.073$ and $wR_2 = 0.123$ for reflections with $I > 2\sigma(I)$, $R_1 = 0.142$ and $wR_2 = 0.140$ for all data.

■ ASSOCIATED CONTENT

■ Supporting Information

Powder X-ray diffraction data for $\text{K}_{12}\text{Si}_8\text{Ge}_9$, $\text{K}_{12}\text{Si}_5\text{Ge}_{12}$ and $\text{Rb}_{12}\text{Si}_8\text{Ge}_9$, EPR spectra of the residue of compound **3** after evaporation of ammonia and for comparison of paramagnetic Cu^{II} obtained by oxidation of PPh_3CuCl , as well as anisotropic displacement parameters for selected atoms in compounds **1**, **2**, **3**, and **4**. X-ray crystallographic files of compounds **1**, **2**, **3**, and **4** in CIF format. This material is available free of charge via the Internet at <http://pubs.acs.org>.

■ AUTHOR INFORMATION

■ Corresponding Author

*Tel.: (+49) 89-289-13131. Fax: (+49) 89-289-13186. E-mail: thomas.faessler@lrz.tum.de.

■ Notes

The authors declare no competing financial interest.

■ ACKNOWLEDGMENTS

The authors thank Prof. Dr. Klaus Köhler, Dr. Carmen Haefner, and Oliver Dachwald for providing the EPR spectrometer and Prof. Dr. Bernhard Rieger and Dr. Sergei Vagin for the possibility to use the ESI mass spectrometer. This work was supported by the SolTech (Solar Technologies go Hybrid) program of the State of Bavaria.

■ REFERENCES

- (1) Abedrabbo, S.; Arafah, D.-E.; Salem, S. J. *Electron. Mater.* **2005**, *34*, 468.
- (2) Waibel, M.; Benda, C. B.; Wahl, B.; Fässler, T. F. *Chem.—Eur. J.* **2011**, *17*, 12928.
- (3) Waibel, M.; Raudaschl-Sieber, G.; Fässler, T. F. *Chem.—Eur. J.* **2011**, *17*, 13391.
- (4) Waibel, M.; Henneberger, T.; Jantke, L.-A.; Fässler, T. F. *Chem. Commun.* **2012**, *48*, 8676.
- (5) Corbett, J. D. *Chem. Rev.* **1985**, *85*, 383.
- (6) Corbett, J. D. *Struct. Bonding (Berlin)* **1997**, *87*, 157.
- (7) Fässler, T. F. *Coord. Chem. Rev.* **2001**, *215*, 347.
- (8) Scharfe, S.; Fässler, T. F. *Philos. Trans.* **2010**, *368*, 1265.

- (9) Scharfe, S.; Kraus, F.; Stegmaier, S.; Schier, A.; Fässler, T. F. *Angew. Chem., Int. Ed.* **2011**, *50*, 3630.
- (10) Wade, K. *Nucl. Chem. Lett.* **1972**, *8*, 559.
- (11) Wade, K. *Adv. Inorg. Chem. Radiochem.* **1976**, *18*, 1.
- (12) Goicoechea, J. M.; Sevov, S. C. *J. Am. Chem. Soc.* **2004**, *126*, 6860.
- (13) Fässler, T. F.; Hunziker, M.; Spahr, M. E. *Z. Anorg. Allg. Chem.* **2000**, *626*, 692.
- (14) Xu, L.; Sevov, S. C. *J. Am. Chem. Soc.* **1999**, *121*, 9245.
- (15) Scharfe, S.; Fässler, T. F. *Z. Anorg. Allg. Chem.* **2011**, *637*, 901.
- (16) Hauptmann, R.; Fässler, T. F. *Z. Anorg. Allg. Chem.* **2003**, *629*, 2266.
- (17) Hauptmann, R.; Fässler, T. F. *Z. Kristallogr. NCS* **2003**, *218*, 461.
- (18) Wang, J.-Q.; Wahl, B.; Fässler, T. F. *Angew. Chem., Int. Ed.* **2010**, *49*, 6592.
- (19) Ugrinov, A.; Sevov, S. C. *J. Am. Chem. Soc.* **2002**, *124*, 10990.
- (20) Yong, L.; Hoffman, S. D.; Fässler, T. F. *Z. Anorg. Allg. Chem.* **2005**, *631*, 1149.
- (21) Ugrinov, A.; Sevov, S. C. *Inorg. Chem.* **2003**, *42*, 5789.
- (22) Yong, L.; Hoffman, S. D.; Fässler, T. F. *Z. Anorg. Allg. Chem.* **2004**, *630*, 1977.
- (23) Downie, C.; Tang, Z.; Guloy, A. M. *Angew. Chem.* **2000**, *112*, 345.
- (24) Downie, C.; Mao, J. G.; Guloy, A. M. *Inorg. Chem.* **2001**, *40*, 4721.
- (25) Karttunen, A. J.; Fässler, T. F.; Linnolahti, M.; Pakkanen, T. A. *Chem. Phys. Chem.* **2010**, *11*, 1944.
- (26) Fässler, T. F. *Angew. Chem.* **2007**, *119*, 2624. Fässler, T. F. *Angew. Chem., Int. Ed.* **2007**, *46*, 2572.
- (27) Guloy, A. M.; Ramlau, R.; Tang, Z.; Schnelle, W.; Baitinger, M.; Grin, Y. *Nature* **2006**, *443*, 320.
- (28) Armatas, G. S.; Kanatzidis, M. G. *Science* **2006**, *313*, 817.
- (29) Quéneau, V.; Todorov, E.; Sevov, S. C. *J. Am. Chem. Soc.* **1998**, *120*, 3263.
- (30) Waibel, M.; Kraus, F.; Scharfe, S.; Wahl, B.; Fässler, T. F. *Angew. Chem., Int. Ed.* **2010**, *49*, 6611.
- (31) Scharfe, S.; Fässler, T. F. *Eur. J. Inorg. Chem.* **2010**, 1207.
- (32) Kocak, F. S.; Downing, D. O.; Zavalij, P.; Lam, Y.-F.; Vedernikov, A. N.; Eichhorn, B. *J. Am. Chem. Soc.* **2012**, *134*, 9733.
- (33) Critchlow, S. C.; Corbett, J. D. *J. Am. Chem. Soc.* **1983**, *105*, 5715.
- (34) Angilella, V.; Belin, C. *J. Chem. Soc., Faraday Trans.* **1991**, *87*, 203.
- (35) Hunziker, M.; Fässler, T. F. *Inorg. Chem.* **1994**, *33*, 5380.
- (36) Hunziker, M.; Fässler, T. F. *Z. Anorg. Allg. Chem.* **1996**, *622*, 837.
- (37) Schütz, U.; Fässler, T. F. *Inorg. Chem.* **1999**, *38*, 1866.
- (38) Joseph, S.; Suchentrunk, C.; Kraus, F.; Korber, N. *Eur. J. Inorg. Chem.* **2009**, 4641.
- (39) Joseph, S.; Suchentrunk, C.; Korber, C. *Z. Naturforsch.* **2010**, *65b*, 1059.
- (40) Fife, D. J.; Moore, W. M.; Morse, K. W. *Inorg. Chem.* **1984**, *23*, 1684.
- (41) Costa, G.; Reisenhofer, E.; Stefani, L. *J. Inorg. Nucl. Chem.* **1965**, *27*, 2581.
- (42) Eriksson, H.; Hakansson, M. *Organometallics* **1997**, *16*, 4243.
- (43) Bowmaker, G. A.; Boyd, S. E.; Hanna, J. V.; Hart, R. D.; Healy, P. C.; Skelton, B. W.; White, A. H. *J. Chem. Soc., Dalton Trans.* **2002**, 2722.
- (44) Werner, H.; Otto, H.; Ngo-Khac, T.; Burschka, C. *J. Organomet. Chem.* **1984**, *262*, 123.
- (45) Scharfe, S. Dissertation, Technische Universität München, Garching, Germany, 2010.
- (46) Chatt, J.; Venanzi, L. M. *J. Chem. Soc.* **1957**, 4735.
- (47) WinXPow, version 2.08; Stoe & Cie GmbH: Darmstadt, Germany, 2003.
- (48) Sheldrick, G. M. *SHELXS-97*; Program for the Solution of Crystal Structures; Universität Göttingen: Göttingen, Germany, 1997.
- (49) Sheldrick, G. M. *SHELXS-97*; Program for the Refinement of Crystal Structures; Universität Göttingen: Göttingen, Germany, 1997.